Arabian Journal of Chemical and Environmental Research

Vol. 07 Issue 2 (2020) 94–125

Review: Synthesis of Crystalline Nanocellulose by Various Methods

A. Haerunnisa[1], D. Ramadhan[1*], H. A. Y. Putra[1], N. Afiifah[1], R. Devita[1], S. Rahayu[1], A. B. D. Nandiyanto[1]

[1]*Departemen Pendidikan Kimia, Fakultas Pendidikan Matematika dan Ilmu Pengetahuan Alam, Universitas Pendidikan Indonesia, Jl. Dr. Setiabudi no. 229, Bandung 40514, Jawa Barat, Indonesia*

Received 18 September 2020, Revised 19 October 2020, Accepted 25 October 2020

Abstract

Crystalline nanocellulose is an important material in supporting the needs of the industrial sector today. Because of its many uses, encouraging researchers to develop crystalline nanocellulose synthesis methods with various treatments and sources. Of the many methods, not all of them can be applied on an industrial scale. Therefore, the author aims to review the literature on the synthesis of crystalline nanocellulose so that we know which methods can be applied on an industrial scale. In this paper, we review 60 papers from 1995 to 2020 then highlight 12 representative recent papers. This review is expected to be a reference in selecting crystalline nanocellulose synthesis methods for industrial use, given the lack of specific reviews on crystalline nanocellulose synthesis for industrial-scale applications. From the results of the review of several papers, the team of authors believes that the synthesis of nanocellulose which is suitable for application on an industrial scale is the acid hydrolysis method. This is based on the findings that with this synthesis, more samples are obtained, the process is more efficient, following current industrial developments and the materials used can be agricultural waste which is rarely seen in the industrial world.

Keywords: Cellulose, Nanocellulose, Crystalline Nanocellulose, synthesis of nanocellulose.

*Corresponding author.
E-mail address: dangboyrama17@upi.edu

1. Introduction

The production of cellulose at the nanoscale has attracted attention because the properties of the resulting material have advantages, such as high strength and hardness combined with its light, biodegradable, and renewable properties [1]. The conversion of cellulose from micro to nano is an effort so that the application of this material is growing [2]. Nanocelluloses are a new class of nanoscale biopolymers that are creating a revolution in biologically based materials for various industrial applications, such as personal care, food chemistry, pharmaceuticals, and biocomposites [3]. Generally, there are three types of nanocellulose, namely crystalline nanocellulose (CNC), cellulose nanofibrils (CNF), and bacterial cellulose (BC) [4]. Nanocelluloses with nanoscale particle size and high crystallinity are commonly used as nanofillers for polymer materials, barriers in hazardous waste separation processes, food packaging that replaces non-biodegradable plastics, and as nanocomposites [5,6].

The material used as a source of cellulose for further processing into crystalline nanocellulose (CNC), generally comes from higher plants such as wood [7], cotton [8],wheat straw [9], coconut husk [10], bamboo fiber [11,12], microcrystalline cellulose (MCC) [13,14], hemp fiber [15], kenaf [16], phormium tenax fiber [17], mengkuang leaf [18], sisal fiber [19], and others. In addition, tunicate (a type of marine animal) [7,20], and bacterial cellulose (BC) [21,22] are also used as a source of cellulose.

Ionic liquids can be used as cellulose solvents with the ability to dissolve depending on the size and polarity of the anions. Ionic liquid anions will make more easily breaking the hydrogen bonds that occur between cellulose molecules. Thus, the process of dissolving cellulose will be faster. It can dissolve cellulose with a higher concentration. The mechanism that occurs is the breaking of hydrogen bonds [23]. The ionic liquid used will interfere with the intermolecular hydrogen bond interactions of cellulose through hydrolysis reactions. The cation will attack the O atom from the –OH group while the anion will attack the H atom from the –OH group. Figure 1 shows an example of the cellulose dissolution mechanism by the ionic liquid Butyl-methylimidazolium chloride ([BMIM] Cl) [24].

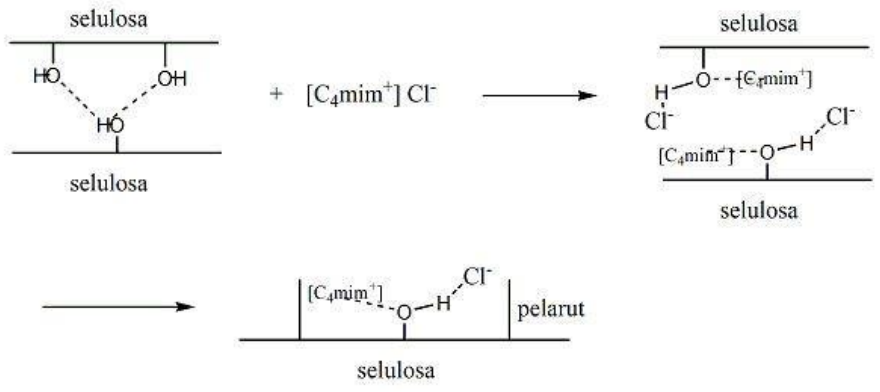

Figure 1. Dissolving cellulose with ionic liquids. Figure adopted from Li et al. [24].

Apart from using ionic liquids, the addition of strong acids is a step to convert cellulose into crystalline nanocelluloses through a hydrolysis reaction [25]. When acid hydrolysis occurs, cellulose which has two parts, namely the crystalline and amorphous parts, will undergo a structural change as a result of the loss of the amorphous part. Figure 2 shows the amorphous removal during the acid hydrolysis reaction leaving a nano-sized cellulose crystal [26].

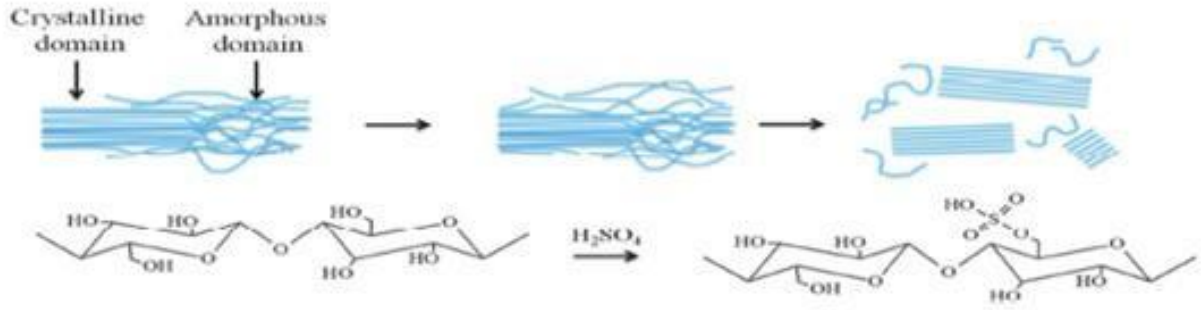

Figure 2. Hydrolysis of strong acids in cellulose. Figure adopted from Ehmann et al. [26].

The amorphous area present in the cellulose chain is the first part and is easily accessible to the acid so that it can be hydrolyzed. However, the presence of kinetic forces and steric resistance in the crystalline region makes this part unaffected by hydrolysis [27,28]. The structure, properties, and phase separation behavior of the crystalline nanocellulose suspension are highly dependent on the type of mineral acid and its concentration, the temperature and time of hydrolysis, and the intensity of the ultrasonic radiation used [29]. There are various methods in the synthesis of crystalline nanocelluloses, namely mechanical methods [26], chemical methods consisting of the acid method [14], the organosolv method [30], the alkaline solvent method [31], oxidation method [32], and the ionic liquid method [33], and biological methods [22]. However, these various synthesis methods are not entirely applicable in industrial nanocellulose synthesis, even though the application of nanocellulose is very beneficial in the various fields that have been mentioned. Therefore, writing this paper aims to determine the synthesis method of crystalline nanocellulose which can be applied on an industrial scale by reviewing 60 papers from 1995 to 2020 then highlighting 12 papers published in the last ten (most recent) years that are representative. As shown in Table 1, the synthesis of crystalline nanocellulose from 12 recent papers used a variety of sources and produced various nanocellulose sizes. The advantages and disadvantages of each method are discussed in more detail in the synthesis method section.

Although there have been many papers discussing the manufacture of nanocellulose, the number of papers that have reviewed the manufacture of nanocellulose, especially crystalline nanocellulose, is still limited. So, it is hoped that this paper can become a reference in the selection of industrial crystalline nanocellulose synthesis methods.

Table 1. Recent studies regarding the synthesis of crystalline nanocellulose from various biomass sources and the size of the resulting nanocelluloses.

Type of Nanocellulose	Material	Method	Result	Reference
Crystalline	Microcrystalline cellulose, 1-butyl-3-methylimidazolium hydrogen sulfate (bmimHSO$_4$)	Hydrolysis of ionic liquids	Nanocellulose 50-300 in size and 14-22 nm in diameter	[33]
	Microcrystalline cellulose, sulfuric acid (H_2SO_4)	Hydrolysis of Acid	Nanocellulose measuring 150-200 and 10-20 nm in diameter	[14]
	Rice Husk, 4 wt% NaOH, buffer solution of acetic acid, dilute chlorite (1.7% by weight), sulfuric acid		Crystalline nanocellulose measuring 15-20 nm and 10–15 nm	[39]
	Oil palm empty bunches, sulfuric acid (H_2SO_4), NaOH 17, 5%, NaOH 17.5% (w / v), H_2O_2 10% (v / v), CH3COOH 10% (v / v),		Nanocellulose measuring 160-298 nm	[44]
	Bark Tree Fronds zalacca, Nitric Acid (HNO_3), NaOH, Na_2SO_3, NaOCl, H_2O_2, H_2SO_4		Nanocellulose measuring 16.52 nm	[47]
	Red Onion Waste, ethanol, distilled water, H_2O_2, and NaOH		Nanocellulose measuring 12.615 nm	[50]
	Corn cobs, aqua dm, sodium hypochlorite, sodium hydroxide, and sulfuric acid		nanocellulose with a diameter range of 14.30-45.00nm and an average diameter of 17.40nm.	[52]
	Eucalyptus pellita fiber, sulfuric acid (H_2SO_4), NaOH, hypochlorite solution		Nanocellulose measuring 82.70nm	[53]

Table 1. (continued) Recent studies regarding the synthesis of crystalline nanocelluloses from various biomass sources and the size of the resulting nanocelluloses.

Type of Nanocellulose	Material	Method	Result	Reference
Crystalline	Lin cotton tar, 2,2,6,6-tetramethyl-pipelidine-1-oxyl (TEMPO)	Oxidation	Nanocellulose with a width of 5-10 nm and a length of 200 to 400 nm	[35]
	Microcrystalline cellulose, nickel (II) nitrate hexahydrate	Hydrolysis of salt catalysts	nanocellulose 300-600 in size and 10-60 nm in diameter	[60]
	Polar wood, phosphoric acid, glacial acetic acid, sodium chlorite, cellulase	enzymolysis-assisted sonication	Nanocellulose 20-50 nm in diameter	[63]
	Cotton fibers, microcrystalline cellulose (MCC), dextrose broth, *Trichoderma reesei* (ATCC 13631), ultrapure water	Microbial hydrolysis of enzymatic	crystalline nano-celluloses produced with deep diameter 100-150 nm range	[34]

2. Synthesis of Crystalline Nanocellulose

To obtain crystalline nanocellulose from biomass, it is generally carried out in three stages, namely (1) removal of lignin and hemicellulose from biomass material by alkaline treatment or addition of dilute strong acids, (2) purification of cellulose by adding buffers, (3) isolation of crystalline nanocellulose by hydrolysis of cellulose by various methods such as the addition of ionic liquids [23], strong acids [26-29], microbial enzymatics [34], and oxidation [35] which are generally followed by sonication, dialysis and, centrifugation. According to Rojas, an overview of the synthesis of crystalline nanocellulose is in accordance with Figure 3 shows the flow of crystalline nanocellulose synthesis from biomass materials [36].

2.1. Hydrolysis of ionic liquids

Man et al. [33] reported the results of the synthesis of crystalline nanocellulose using the hydrolysis method with 1-butyl-3-methylimidazolium hydrogen sulfate ($bmimHSO_4$) as a catalyst and microcrystalline cellulose (MCC) as a source of cellulose. Ionic liquids similarly react with MCC acid

hydrolysis. Ionic liquid causes hydrolytic cleavage of the glycosidic bonds between two anhydroglucose units and result in rearrangements of the linked ends of the chains, which facilitate the release of internal strain [37,38]. Ionic liquids dissolve the amorphous and leave behind the crystalline regions. Treatment with ionic liquids with mechanical stirring resulted in the disintegrated of the microcrystalline cellulose structure into crystalline nanocellulose particles [33].

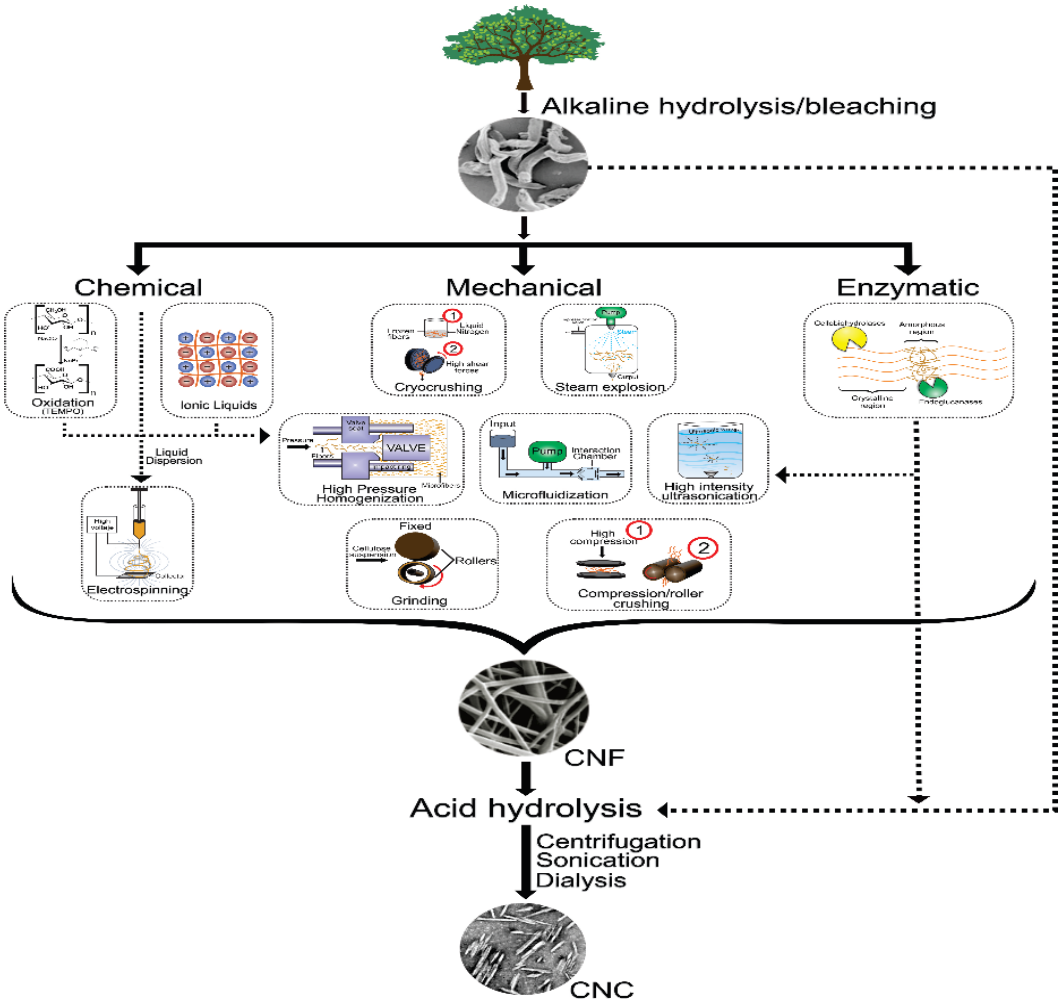

Figure 3. The flow crystalline nanocellulose synthesis (CNC). Figure adopted from Rojas et al. [36]

MCC 10% (w/w) was mixed with bmimHSO$_4$ and treated for 1 hour at 70, 80 and, 90 °C with each stirring speed of 400 rpm. The mixture is sonicated at room temperature, and the suspension is washed with deionized water several times using centrifugation at 2,000 rpm for 15 minutes. The supernatant obtained was centrifuged at 7,500 rpm for 30 minutes until crystalline nanocellulose particles were obtained [33]. MCC dissolution did not occur during treatment with ionic liquids. From diffractogram on Figure 4 shows that no change in the type of cellulose before and after MCC was treated with bmimHSO$_4$. Figure 5 shows the increase in the crystallinity index is respectively the increase in temperature.

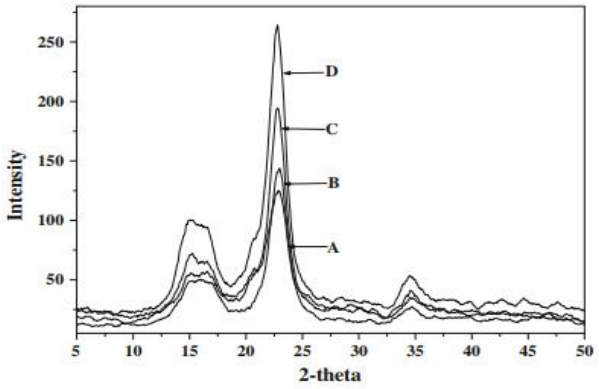

Figure 4 . XRD diffractogram of MCC (A) and crystalline nanocelluloses at heating temperatures (70, 80, and, 90 ° C), were heated for 1 hour. Figure adopted from Man et al. [33].

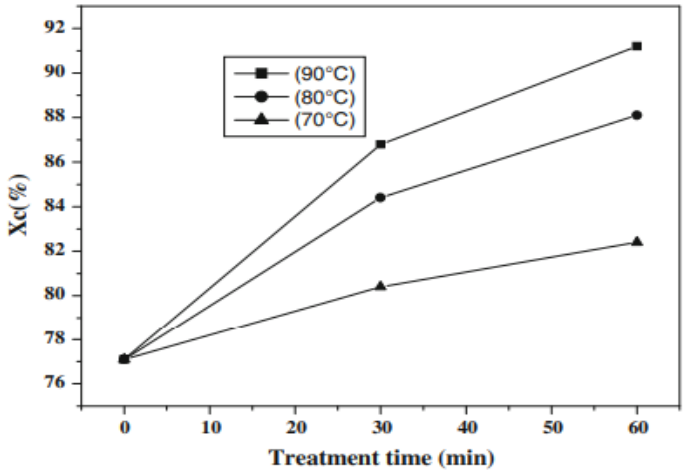

Figure 5. The crystallinity index of microcrystalline cellulose and crystalline nanocellulose after treatment at different times. Figure adopted from Man et al. [33].

FTIR analysis showed that the MCC and crystalline nanocellulose obtained after treatment with bmimHSO$_4$ had the same basic structure, shown in Figure 6. This spectrum confirms that bmimHSO$_4$ does not change during treatment, so it can be recycled [33].

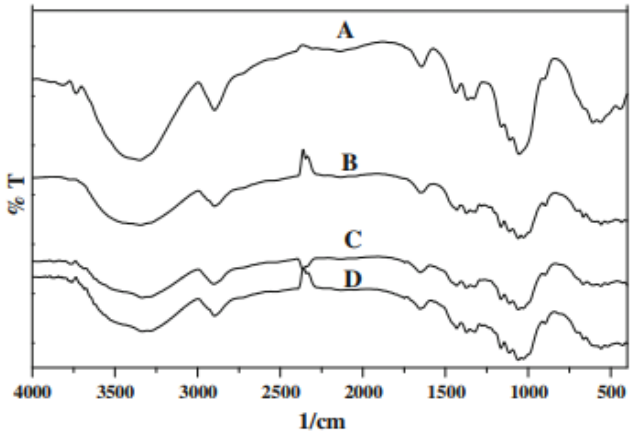

Figure 6. FTIR spectra of MCC (A) and crystalline nanocelluloses at different heating temperatures (T = 70 °C, t = 1 hour), (T = 80 °C, t = 1 hour), (T = 90 °C, t = 1 hour). Figure adopted from Man et al. [33].

The crystalline nanocelluloses produced by Man et al. [33] are 50-300 x 14-22 nm in size with a needle-like structure obtained at three different temperatures as shown in Figure 7. The size of crystalline nanocellulose decreases as the heating temperature is increased during hydrolysis, where the smallest size of crystalline nanocelluloses is shown in Figure 7c.

Needle-like structure of crystalline nanocellulose with a diameter of 21.42 nm at the center and tapered to 13.38 at the end obtained from crystalline nanocellulose at 90 ℃ for 1 hour. The Transmission Electron Microscope (TEM) is shown in Figure 8.

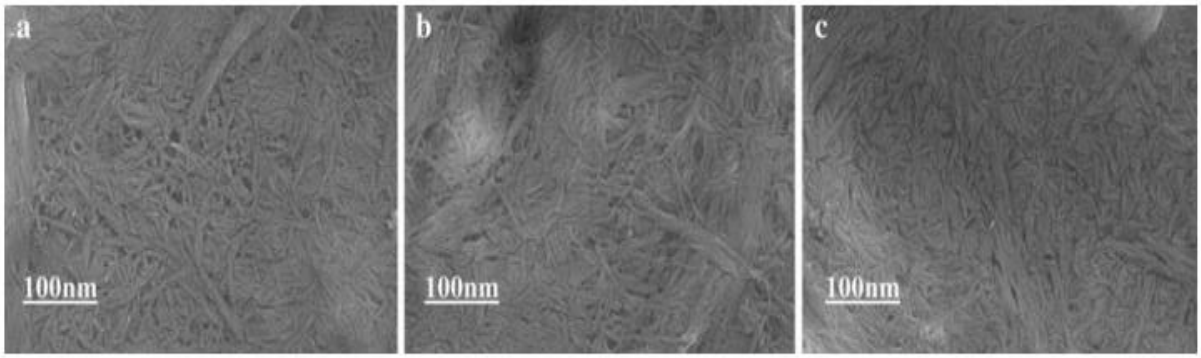

Figure 7. FESEM (50.00 KX) of crystalline nanocellulose at different heating temperatures (T = 70 ° C, t = 1 hour), (T = 80 ° C, t = 1 hour), (T = 90 ° C, t = 1 hour). Figure adopted from Man et al. [33].

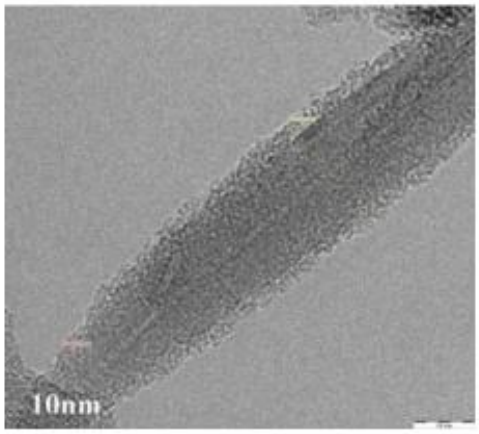

Figure 8. TEM micrograph of crystalline nanocellulose at 90 ° C for 1 hour. Figure adopted from Man et al. [33]

2.2. Hydrolysis of Acid

2.2.1. Microcrystalline Cellulose with Sulfuric Acid

Ioelovich [14], synthesized nanocellulose with cellulose from microcrystalline cellulose (MCC) which was hydrolyzed with sulfuric acid (H_2SO_4) at various concentrations around 50-67% wt and the ratio of acid to cellulose (ACR) from 5-20. The reaction temperature used was 40-60 ℃, with a centrifugation stirring speed of 3200 rpm. Figure 9 shows the X-Ray Diffraction (XRD), with sulfuric acid

concentrations in the range from 55-62% wt, it was found that the nanocellulose particles maintained a crystallinity similar to the microcrystalline cellulose. When the sulfuric acid concentration is more than 63% by weight, microcrystalline cellulose dissolves in sulfuric acid, as a result, the crystallinity of the particles is low [14]. Crystalline nanocellulose isolated with sulfuric acid 60% wt, having a rod-like shape with a size of 150-200 x 10-20 nm was confirmed using Scanning Electron Microscope (SEM) shown in Figure 10. When the sulfuric acid concentration was more than 63% wt, the nanocellulose was obtained an amorphous ellipsoidal with a wide size distribution from 50 to 300 nm shown in Figure 11.

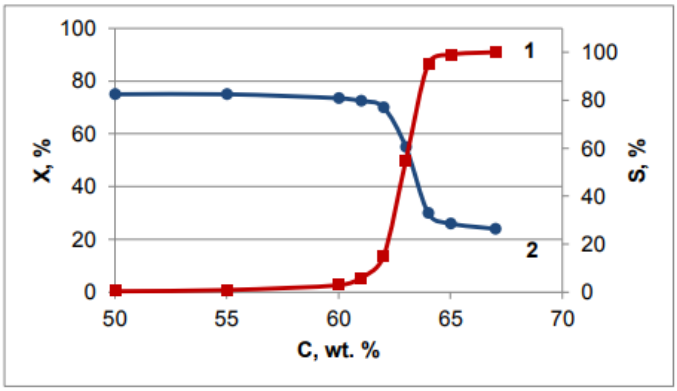

Figure 9. Dependence of solubility of cellulose (1) and degree of crystallinity (2) of isolated nanocellulose on sulfuric acid concentration. Figure adopted from Ioelovich [14].

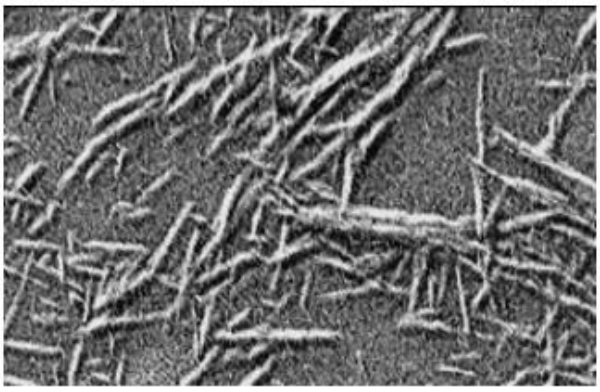

Figure 10. SEM crystalline nanocellulose particles using sulfuric acid 60% wt. Figure adopted from Ioelovich [14]

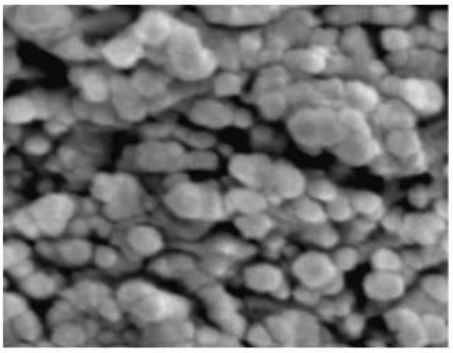

Figure 11. SEM of amorphous cellulose ellipsoidal nanoparticles when the sulfuric acid concentration was over 63%. Figure adopted from Ioelovich [14].

2.2.2. Hydrolysis of sulfuric acid in rice husks

Johar et al. [39] synthesized crystalline nanocellulose from rice husk material. First, an alkaline treatment is carried out to purify the cellulose by removing lignin and hemicellulose [39,40]. The resulting solid is filtered and washed several times using distilled water, repeated three times [39]. The mixture is allowed to cool and filtered using distilled water. excess. The bleaching process was repeated four times [39]. The next process is acid hydrolysis carried out after alkaline treatment and bleaching. The hydrolysis process takes place at a temperature of 50 °C, sulfuric acid 10.00 M. This centrifugation step is repeated several times before the suspension is dialyzed with distilled water for several days until a constant pH in the range of 5-6 is reached. [39]. The first characterization is chemical content. Figure 12 shows a photograph of the husk fiber without treatment, after alkaline treatment and bleaching. The difference in form indicates a change in chemical composition [39,41].

Figure 12. Photography of rice husk, **Figures 12** (a), (b), and (c) are rice husk without treatment, rice husk treated with alkaline, and rice husks that have received alkaline and bleaching treatment, respectively. Figure adopted from Johar et al. [39].

The next characterization is Scanning Electron Microscope (SEM). The effect of the bleaching treatment can be observed from the comparison of after alkaline treatment shown in Figure 13b and after the bleaching treatment shown in Figure 13c. It can be observed that the fiber bonds of the rice husk are separated into individual fibers. The diameter of the fibrous material decreased from an average of about 170–7 μm. This reduction indicates that alkaline treatment cannot destroy the natural bundles of cellulose [39,42]. Therefore, the required bleaching is to destroy the natural bundles of cellulose so that the rice husks break down to form cellulose microfibrils [39].

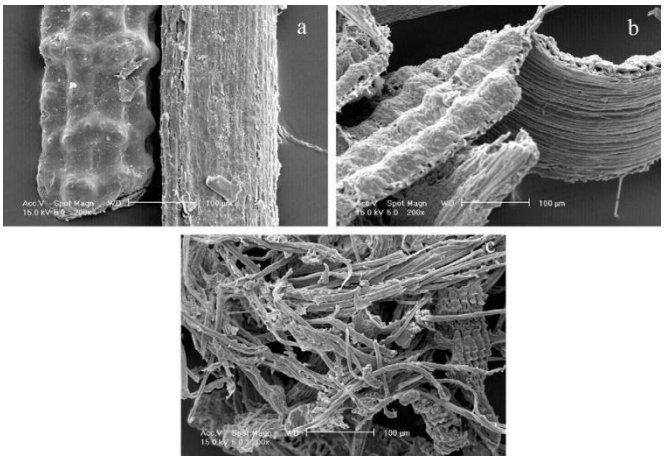

Figure 13. Rice husk morphology through SEM analysis. Figures 13 (a), (b), and (c) are the morphology of rice husks without treatment, rice husks undergoing alkaline treatment, and rice husks undergoing alkaline and bleaching treatment, respectively. Figure adopted from Johar et al. [39].

Then the analysis was performed by the Transmission Electron Microscope (TEM). Figure 14A shows the results of the TEM analysis of crystalline nanocellulose from acid hydrolysis. Acid hydrolysis using sulfuric acid under controlled conditions aims to remove amorphous portions of cellulose microfibrils [39,42]. Johar et al. [39] also reported that the diameter of crystalline nanocellulose and the aspect ratio of crystalline nanocellulose respectively are shown in Figure 14B. Most nanoparticles display a range of 15-20 nm and 10–15 nm.

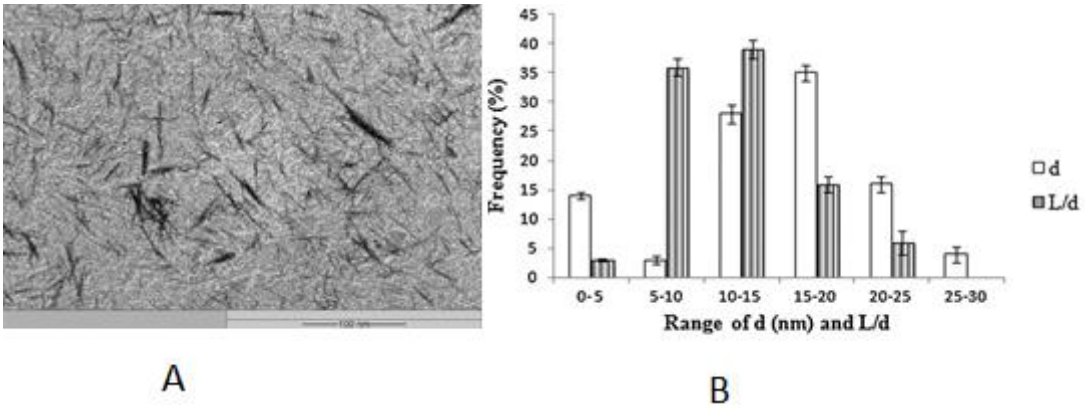

Figure 14. **(A)** Morphology of crystalline nanocellulose through TEM analysis **(B)** Diameter and aspect ratio of CNC extracted from rice husk fiber. Figure adopted from Johar et al. [39].

Synthesis of CNC from rice husks using the methods and steps that have been carried out such as alkaline treatment, bleaching, and sulfuric acid hydrolysis has the advantage of being able to increase the cellulose content obtained by alkaline treatment and bleaching [39], increasing the crystallinity index [28,39]. Johar et al. [39] reported that the synthesis of CNC from rice husks using this method produced CNCs with a diameter of 10–15 nm.

2.2.3. Acid hydrolysis in empty oil palm bunches.

This study aims to characterize the isolated nanocrystals from empty oil palm bunches. The process used was lignification with 3.5% HNO_3 and $NaNO_2$, and pulping with 17% NaOH. In the pulping process, the fibers develop so that the hemicellulose, mineral salts, and ash are lost. The result of this process is a brownish yellow pulp [43]. The next step was bleaching with 10% H_2O_2 and the last one was the isolation of the nanocrystals using the acid hydrolysis method with 48.84% H_2SO_4 [44]. During the hydrolysis process with 48.84% H_2SO_4, esterification of the hydroxyl group of cellulose with negatively charged sulfate ions occurred on the surface of the cellulose crystals so that the crystal suspension was stable. Hydrolysis with sulfuric acid does not alter the functional groups of cellulose, but only discontinues the glucose ring [45]. Figure 15 shows the results of characterization using FTIR. Figure 16 shows the results of the morphological analysis using TEM.

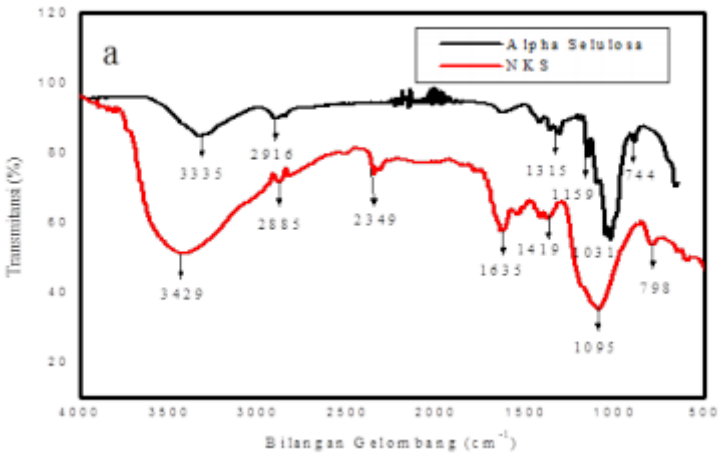

Figure 15. FTIR Spectrum of α-Cellulose and Crystalline Nanocellulose. Figure adopted from Putri et al. [44].

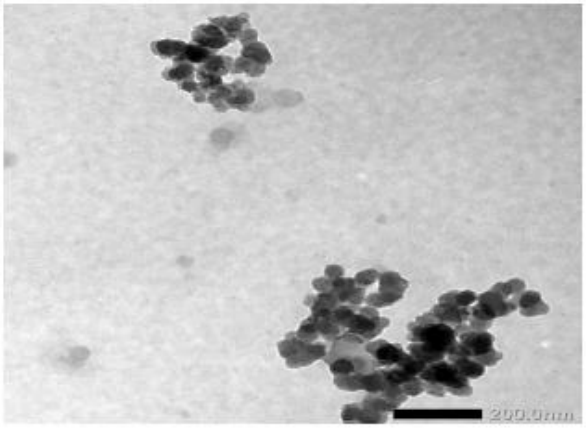

Figure 16. Morphology of Crystalline Nanocellulose Using TEM. Figure adopted from Putri et al. [44].

The FTIR spectrum shows a band widening in the area of 3000-4000 cm^{-1} wave number which is the vibration of the OH bond from cellulose, and at the wave number 800-1300 cm^{-1} is the vibration of the CO bond, and there is an absorption band at 700-900 cm^{-1}. This is a bond of β-glycosidic between the

glucose units of cellulose, and the Crystalline Nanocellulose from the resulting empty oil palm bunch has sizes ranging from 46.19–48.73 nm. The resulting Crystalline Nanocellulose were needle crystals based on morphological and size analysis using TEM. Crystalline Nanocellulose had a particle size of 47.46 nm [44]. The strengths of this research are using waste material so that it can reduce the impact of waste. Meanwhile, it lacks a fairly long and lengthy process because it can take 1 to 8 days.

2.2.4. The hydrolysis of sulfuric acid on the fiber material of the bark zalacca tree.

Triyastiti et al. [47] reported the results of the synthesis of crystalline nanocellulose from the bark tree of zalacca which is a source of α cellulose obtained by alkaline treatment using 2% NaOH and continued with the bleaching process with add 1.75% NaOCl solution at boiling point for 30 minutes. Then the α cellulose purification process was carried out by adding 17.5% NaOH solution at 80 ° C for 30 minutes [46]. Furthermore, acid hydrolysis was carried out using H_2SO_4 with a concentration of 40% (v / v) and centrifuged at a speed of 12000 rpm for 5 minutes until neutral. [47].

The FTIR results in Figure 17 shows the appearance of a typical cellulose uptake at the wave number 894 cm^{-1}, which indicates the presence of a CH group (near 900 cm^{-1} refers to close to CH) indicating the presence of β1,4-glycoside bonds between glucose units in cellulose [2,48].

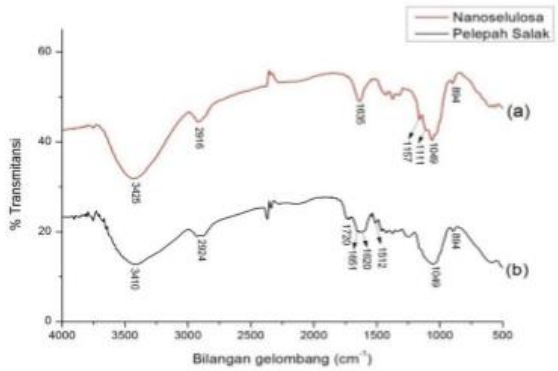

Figure 17. FTIR spectra of (a) nanocellulose (b) bark tree of zalacca**.** Figure adopted from [47].

The X-ray diffraction pattern of the bark tree of zalacca and nanocellulose fractions can be seen in Figure 18. Based on the image, it is known that two distinctive peaks, in nanocellulose, are at an angle of 2θ around 15.4 ° and 22.3 °. These angles are in accordance with JCPDS 50-2241 data which shows the diffraction of cellulose at an angle 2θ 15.0 ° and 22.8 °. Crystallinity was calculated using the segal method and the resulting crystallinity of nanocellulose was 58.42% and bark tree of zalacca 43%. The increase in crystallinity was caused by a decrease in the composition of the amorphous fibers due to acid hydrolysis treatment. The crystal size of cellulose and nanocellulose using the Scherrer equation is 21.09 nm and the crystal size of cellulose is 16.52 nm. The change in size is also caused by the acid hydrolysis process. Apart from acid hydrolysis, ultrasonication is also used to reduce the size of nanocellulose [49].

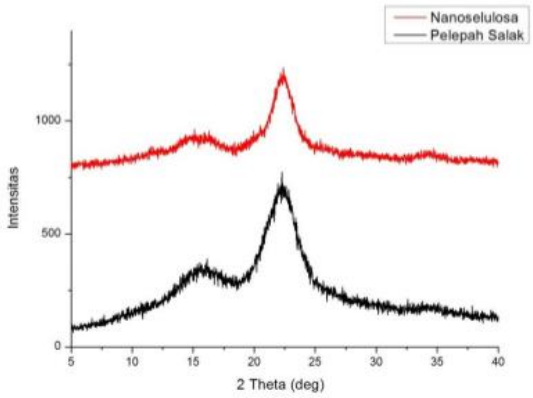

Figure 18. Diffractogram (top) nanocellulose (bottom) bark tree of zalacca. Figure adopted from Triyastiti et al. [47]

Observation of the morphology of the bark tree of zalacca and nanocellulose carried out with an electron microscope can be seen in Figure 19. The fronds still have a fairly large size of around 400 µm due to a simple crushing process by milling. Chemical and mechanical treatments applied to the bark tree of zalacca resulted in a smaller size of about 4 µm. Based on its shape, cellulose nanocellulose produced from this study can be classified as crystalline nanocellulose. This is supported by XRD results which show the crystallinity of nanocellulose exceeds 50% [47].

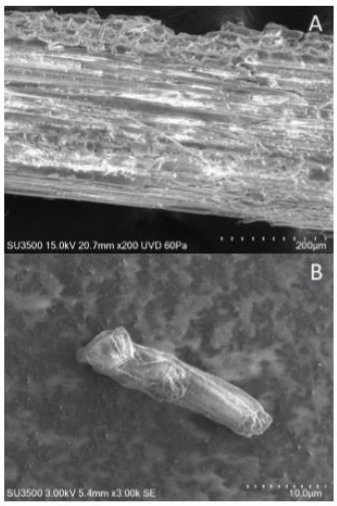

Figure 19. Morphological observations by SEM (A) bark tree of zalacca and (B) Nanocellulose. Figure adopted from Triyastiti et al. [47].

2.2.5. Hydrolysis of Sulfuric Acid in Red Onion Skin Waste

The method used is the extraction of shallot using ethanol, distilled water, H_2O_2, and NaOH. The next step is sample preparation by acid hydrolysis using 50% sulfuric acid. Then the delignification is the process of removing lignin from the onion skin. Delignification was initiated by heating for 2 hours with ethanol and water [50]. Delignification is a process that aims to remove components other than cellulose in cellulose of oil palm empty bunches with alkaline treatment. The type of alkaline solution used is the NaOH solution. NaOH was chosen because it can damage the crystalline structure of lignin and the

amorphous structure of hemicellulose so that these two compounds can be separated from the long carbon chain bonds contained in the fiber [51].

The result of this heating is obtained by the onion skin without wax. After heating, the skin of the onion without wax will be bleached using a sulfuric acid solution using a magnetic stirrer. Then the onion skin is washed with an ethanol-water mixture to remove all lignin and raise the pH. The results of this washing obtained a blackish-brown filtrate and a residue, namely soft red onion skin. Table 2 shows the next step is to re-extract it to get nanocellulose using the same ingredients when extracting the onion. This study varied the heating time and stirring time [50].

Table 2. Comparison of residual yield by varying heating time and stirring time. Table adopted from Sanjaya [50]

Duration of Heating	Duration of Stirring	Residue	Filtrate
1 hour	1 hour	Yellowish white (+++)	Brownish-yellow (+++)
1 hour	2 hour	Yellowish white (++)	Brownish-yellow (++)
2 hour	1 hour	Yellowish white (++)	Brownish-yellow (++)
2 hour	2 hour	Yellowish white (+)	Brownish-yellow (+)

The best method to analyze is when heating and stirring for 2 hours each because the residue is not too yellow compared to the results of the the heating and other stirring. The residual color that is yellow to brownish indicates that the lignin is high enough that it will affect the results because it will produce unwanted quinone compounds. Next is the characterization stage with SEM (Scanning Electron Microscope) and XRD (X-Ray Diffraction). Before being characterized, the sample must be dried first using filter paper and then in an oven at low temperature. After heating at low temperature, the samples were obtained in the form of powder [50]. Figure 20 shows the results of the XRD analysis.

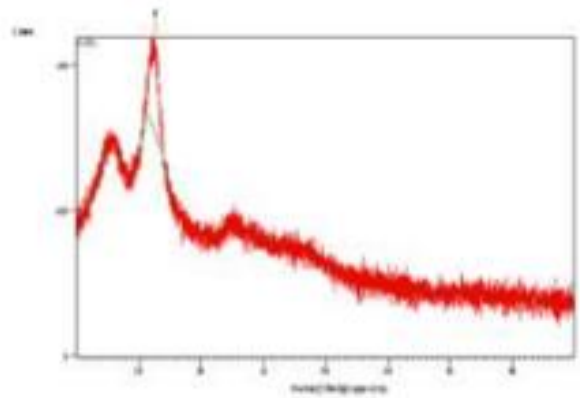

Figure 20. Results of XRD nanocellulose on shallot peel waste. Figure adopted from Sanjaya [50].

The nanocrystalline morphological test is shown in Figure 21, it can be seen that there is a decrease in size before treatment and after treatment. The results of the characterization of XRD obtained a crystallinity index of 78.668%. The shape of the nanocellulose as seen in Figure 21 looks lumpy and uneven. The result of this characterization is a nanocrystalline measuring 12,615 nm. This method uses the acid hydrolysis method to obtain nanocellulose so that the time needed is faster than other methods. In this study, the error occurred when the duration of heating and stirring was too fast at the cellulose extraction stage so that the residue was still yellowish white. This shows that there is still lignin so that when characterized it is still clotted [50].

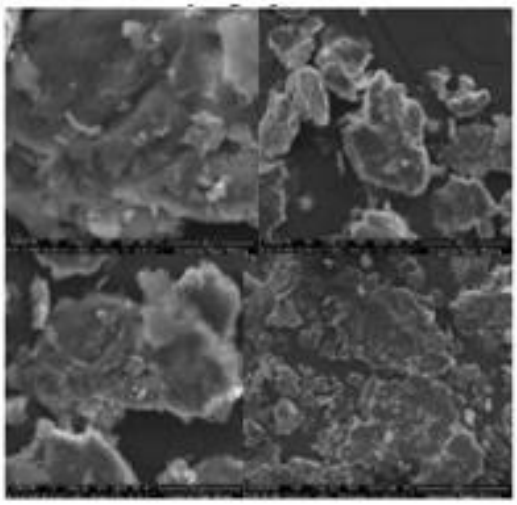

Figure 21. Results of the Scanning Electron Microscope for nanocellulose from shallot peel waste. Figure adopted from Sanjaya [50].

2.2.6. Hydrolysis of sulfuric acid on corncob

Purwanti et al. [52] synthesized crystalline nanocellulose from corncob which is a source of α cellulose obtained by bleaching using 600 mL 1.7% NaOCl. Then performed hydrolysis using sulfuric acid 50% and 60%. Figure 22 shows the results of the TEM analysis. The results of TEM analysis (a), the resulting particle image is not good and the shape of the crystalline nanocellulose particles is not clear, so it is not continued to the next stage. The results of TEM analysis (b) show that the crystalline nanocellulose has a more uniform particle shape and size than the isolated cellulose, which is round [52].

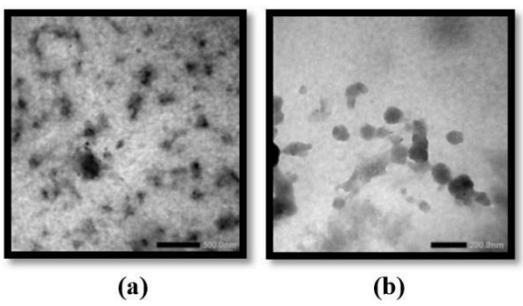

Figure 22. TEM results of crystalline nanocellulose (a) CNC and (b) CNC 60. Figure adopted from Purwanti et al.[52]

2.2.7. Acid hydrolysis method Homified fiber *Eucalyptuspellita* Pandiangan.

The method used is hornification and acid hydrolysis using H_2SO_4 45%. After that the fiber that has been obtained is then centrifuged to produce a pH of 5-6. The fiber is then dialysis using the core membrane (dialysis tubing) until a constant pH is produced. After that the sample is sonicated and autohydrolyzed [53]. In testing using SEM, the shooting results were obtained as below. In Figure 23, a crystalline nanocellulose is shown whose fibers have been fibrillated so that the fiber size shrinks to a nano-scale size. Figures 23a and 23b show a more even and homogeneous surface morphology due to the destruction of a combination of acid hydrolysis, ultrasonication, and autoclave on the sample so that the surface is smoother and homogeneous [53].

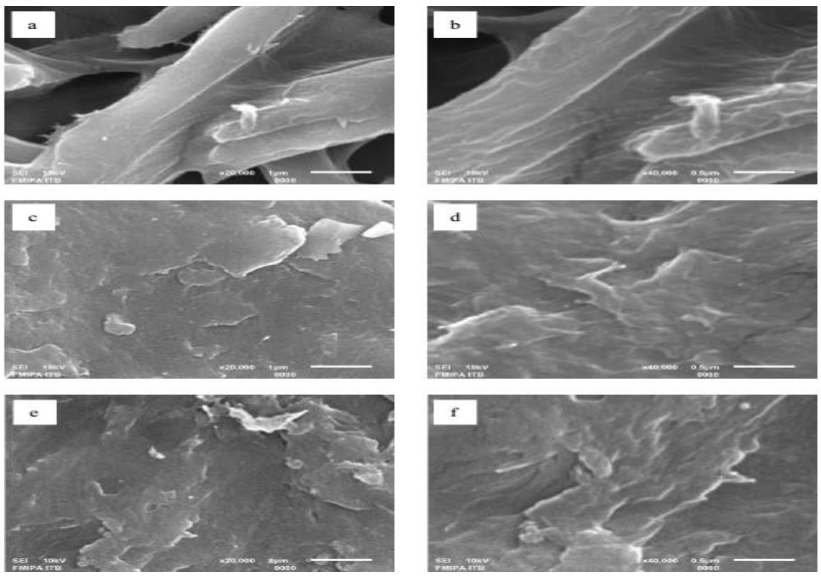

Figure 23. Autohidrolysis Bleaching Hornification 20,000 X magnification (a) Autohidrolysis Bleaching Hornification 40,000 X magnification (b) Autohydrolysis Bleaching 20,000 X magnification (c) Autohidrolysis Bleaching 40,000 X magnification (d) Hydrolysis Bleachingmagnification 20,000 X(e) Hydrolysis Bleaching 40,000 X magnification (f) . Figure adopted from Pandiangan [53].

Figure 24 shows that there are differences in the surface morphology of the samples pulp and after treatment bleaching and chemical modification, namely hornification. The surface of the morphology pulp looks dirty and clumped as shown in Figures 24e and f. However, after hornification, the surface morphology of the fibers was clearer because there was no longer clumping and no impurities as shown in Figures 24a and b. XRD analysis was also carried out to determine the crystallinity of Crystalline Nanocellulose. The percentage of crystallinity of nanocellulose is presented in Table 3 below. The change in the crystal peak when the test was carried out showed the crystallinity value of the fiber nanocellulose *E. pellita* can be seen in Figure 25. If the size of the crystal atom is getting smaller it indicates that the more crystalline structure is indicated by the high crystallinity value. The results obtained in testing the size of the crystallinity tended to be slightly reduced from the samples that had been treated with acid hydrolysis and those that were not acid hydrolyzed (Table 3).

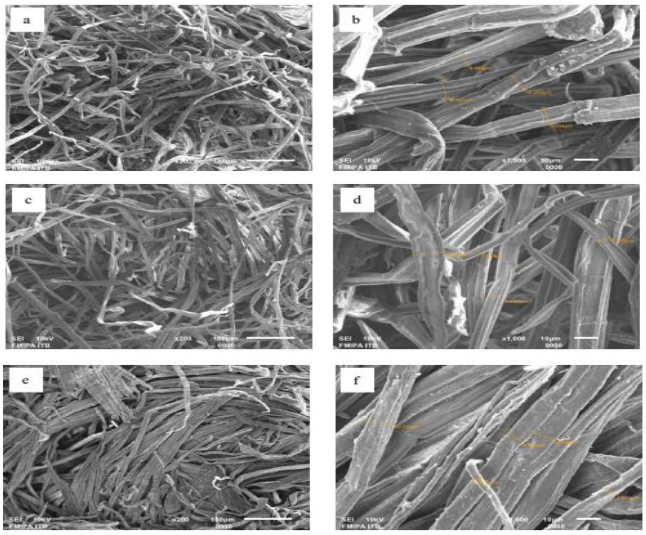

Figure 24. Pulp Bleaching Hornification 100x magnification (a) Pulp Bleaching 2000x magnification (b) Pulp Bleaching 100x magnification (c) Pulp Bleaching 2000x magnification (d) Pulp 100x magnification (e) 200x enlargement pulp (f). Figure adopted from Pandiangan [53].

Table 3. Measures of Crystalline Nanocellulose Crystallinity. Table adopted from Pandiangan [53].

Sample	Crystallinity %
Pulp	58.13
Pulp Bleaching	59.84
Pulp Bleaching Hornification	59.12
Hydrolysis Bleaching	52.94
Autohidrolysis Bleaching	48.57
Autohidrolysis Bleaching Hornification	46.96

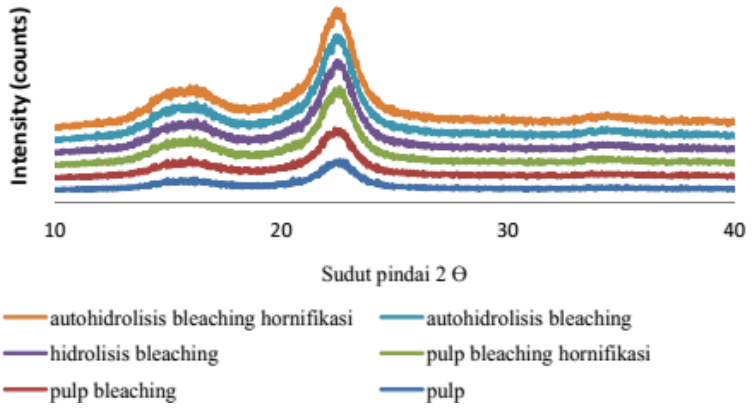

Figure 25. XRD diffractogram. Figure adopted from Pandiangan [53].

The decrease in the crystallinity value is thought to be due to the use of a long time during the acid hydrolysis process so that it can damage the cellulose crystals too. Treatment of the acid hydrolysis can penetrate local goto amorphous cellulose thus causing the hydrolytic cleavage of glycosidic bonds and

release the crystal [54]. The use of FTIR analysis is also performed to determine the functional group of fibers *E. pellita* and nanocellulose, and its changes after being given treatment. The resulting nanocellulose powder then generated characterized so that the results of infrared spectroscopy using FTIR are shown in Figure 26.

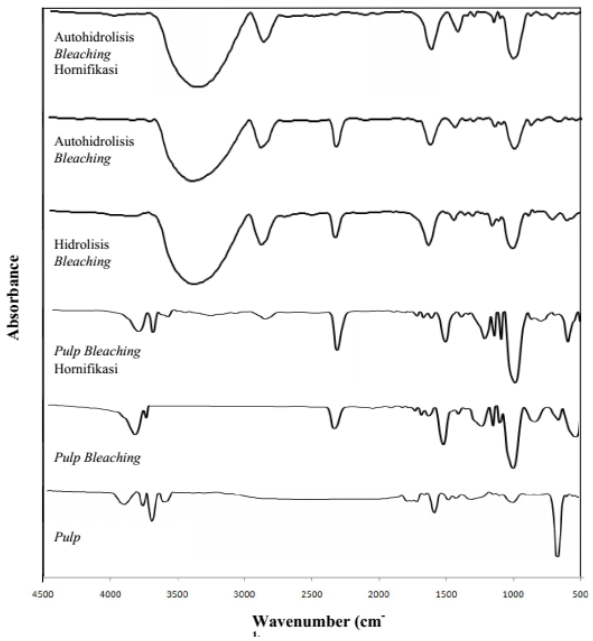

Figure 26. FTIR Spectrum Atohidrolysis Bleaching Hornification, Atohidrolysis Bleaching, Hydrolysis Bleaching, Pulp Bleaching Hornification, Pulp Bleaching, and Pulp. Figure adopted from Pandiangan. [53].

The peak change was seen in the autohydrolysis hornification sample bleaching. Figure 26 shows there are two waves that change, there is the same wave peak in the autohydrolysis sample bleaching with hydrolysis bleaching 2731 cm^{-1} but in the bleaching hornification autohydrolysis, the crest of the wave disappears and a decrease in the peak is seen 1651 cm^{-1} to 1636 cm^{-1} on autohydrolysis of bleaching hornification. Visible pure compound in a changing wave due to purification repeated on autohydrolysis bleaching hornification [55]. So this thing stated by G. Jayme in Minor that hornification is a treatment of drying and soaking cellulose repeatedly to reduce the level of ability of the fiber to expand when soaked with water [56]. The change of each carbon group peak is influenced by changes that occur in the content of lignin, cellulose, and hemicellulose. Thus, this was conveyed in the research of Solikhin et al. [57] that the peak change in each fiber treatment is due to the vibration stretching of cellulose, hemicellulose, and lignin and the occurrence of deformation CH from cellulose and lignin.

2.3. Chemical Oxidation

The oxidation method can be used to synthesize crystalline nanocellulose, which this method is usually used to increase the performance of the alkaline solvent method. The solvent will reduce superoxide

radical (-O_2) at pH > 12 where the aromatic ring of lignin and part of the hemicellulose polymer will be attacked and turn into carboxylic acid compounds [32]. The oxidation method is one of the crystalline nanocellulose synthesis methods that is rarely used because the cost of the material required is quite expensive. And also, the process is quite long and less efficient, because the oxidation method can work optimally when combined with the alkaline solvent method before treatment [58].

Qin et al. [35] reported the results of their research, that is the synthesis of crystalline nanocellulose using the oxidation method with source of the cellulose are linter cotton and an oxidizing agent, 2,2,6,6-tetramethyl-pipelidine-1-oxyl (TEMPO) [35]. Montanari et al. [59] used the same oxidizing reagent in synthesizing nanocellulose. In the process of making nanocellulose, the base material is dispersed using an oxidizing reagent, by adjusting the pH when and after the oxidation, oxidized fibers can be obtained. Ultrasonication with an amplitude of 80 for different periods of 60 and 120 minutes was used so that nanocellulose was obtained [35].

Nanocellulose was present in dilute samples (diluted to 0.1%) after 13.5 hours of being oxidized by TEMPO by the ultrasonic system. Figure 27 shows the crystalline nanocellulose has a width of 5-10 nm and a length of 200-400 nm. With the help of ultrasonics, the oxidized nanocellulose can have more hydrophilic carboxylate groups, which provides more stability to the nanocellulose and allows it to be well dispersed in an aqueous solution [35].

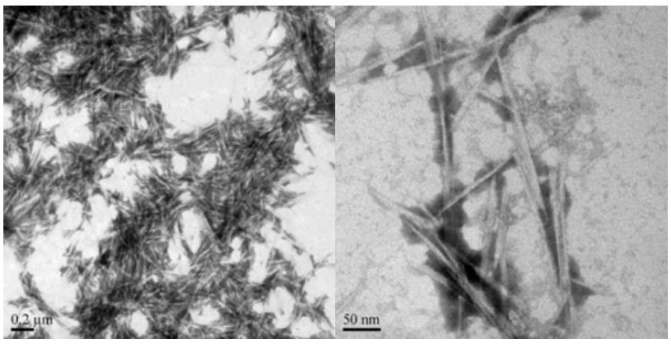

Figure 27. TEM of crystalline nanocellulose with TEMPO. Figure adopted from Qin et al. [35].

2.4. Hydrolysis of Transition Metal Salt Catalysts

Yahya et al. [60] synthesizing microcrystalline cellulose (MCC) through the Ni Transition Metal Salt Catalyst Hydrolysis Pathway with nickel (II) nitrate hexahydrate ($Ni(NO_3)_2.6H_2O$) as the chemical reagent used. The concentration of this chemical reagent has an important role in the synthesis process so that various concentrations are made. Ni-inorganic salt is able to control selectively hydrolysis compared to the sulfuric acid reaction even though low acid concentrations are used.

The main crystalline structure of MCC was maintained and unchanged during the Ni salt catalyst hydrolysis process. When the Ni salt concentration increased from 0.05 to 1.00 M, the intensity of the

XRD diffraction field increased, becoming higher than that of MCC. Figure 28 shows the increase in the crystallinity index and crystal size of nanocellulose treated Ni was positively influenced by the hydrolysis process. Based on the crystallinity profile, the crystallinity index of the samples was in the order MCC <NTC0.05 <NTC0.50 <NTC1.00, indicating an increase of about 5% of the raw material. An increase in the crystallinity index of the treated samples showed significant removal of amorphous regions and increased exposure to cellulose crystalline regions [60].

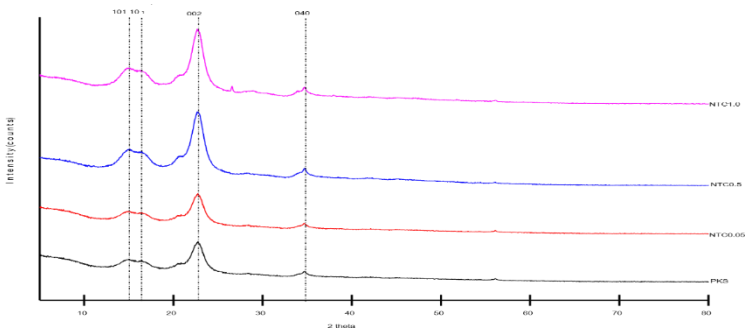

Figure 28. X-ray diffraction patterns of (a) NTC1.0, (b) NTC0.5, (c) NTC0.05, and (d) MCC. Figure adopted from Yahya et al. [60].

The four samples have a similar FTIR pattern, Figure 29 shows the chemical structure of the synthesized nanocellulose remained unchanged after Ni catalyzed hydrolysis. Furthermore, the absence of NO_3^- peaked at 1384 cm^{-1} showed that the Ni salt was completely removed during the washing and dialysis processes [61,62].

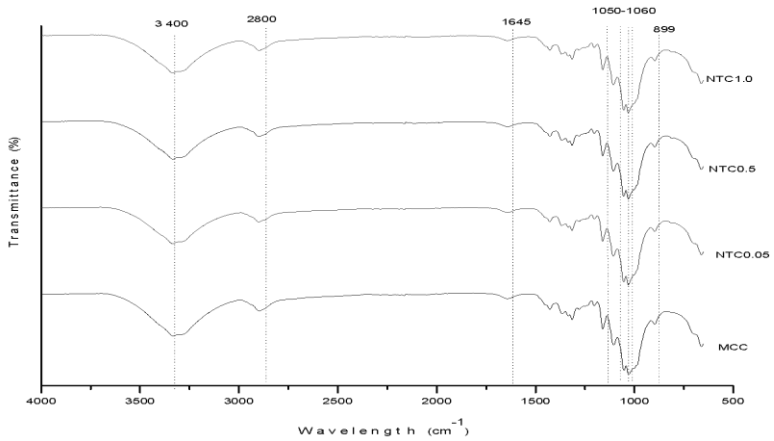

Figure 29. FTIR spectrum from MCC, NTC0.05, NTC0.50, and NTC1.00. Figure adopted from Yahya et al.[60]

The surface morphology of MCC and Ni-treated nanocellulose was determined using field emission scanning electron microscopy (FESEM) analysis. When Ni concentration increases, Ni^{2+} ions spread to the surface of the cellulose fibers and attack the glycosidic bonds of the cellulose chains. Figure 30 shows damage to the amorphous portion of the cellulosic fiber, resulting in smaller particle size and higher fiber porosity [60].

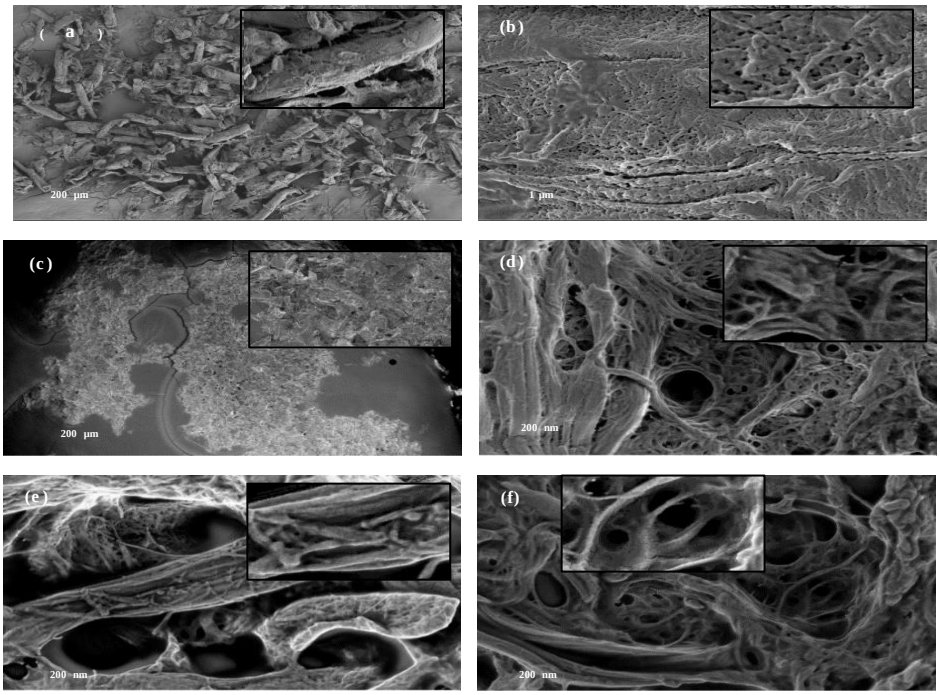

Figure 30. FESEM images of (a) MCC (100 ×), (b) PKS (20000 ×), (c) NTC0.05 (100 ×), (d) NTC0.05 (20000 ×), (e) NTC0.5 (20000 ×), and (f) NTC1.0 (20000 ×). Figure adopted from Yahya et al. [60].

TEM images of Ni-treated nanocellulose with various Ni concentrations is shown in Figure 31. Ni salt catalyzed hydrolysis produces individual Crystalline Nanocellulose in a porous tissue with a spiderweb-like structure. Furthermore, the nanocellulose is expressed in fine diameter (10 to 60 nm) and length at 300 to 600 nm, which implies that Ni ions successfully diffuse into the MCC rigid structure and result in selective fragmentation of the crystals into smaller sizes [60].

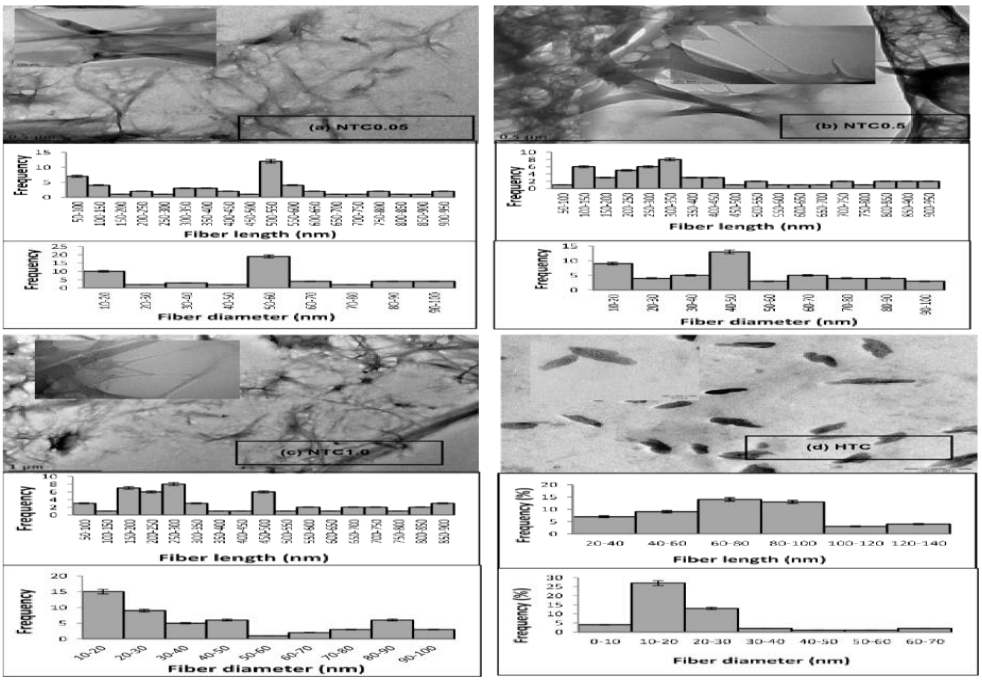

Figure 31. TEM micrographs and Particle Size Distribution Profiles from (a) NTC0.05, (b) NTC0.50, (c) NTC1.00, and (d) HTC. Figure adopted from Yahya et al. [60].

2.5. Enzymolysis-Assisted Sonication

Zhang et al. [63] synthesize Crystalline Nanocellulose from poplar wood through sonication assisted by enzymolysis with cellulase enzymes as surfactants. Most of the hemicellulose and some of the lignin in poplar wood were removed after steam explosion treatment. Sodium chlorite treatment removes nearly all of the remaining lignin and hemicellulose. The yield of Crystalline Nanocellulose depends on the enzyme dose shown in Figure 32. At low doses, most of the cellulose remains, resulting in low yields. With increasing enzyme dose, the yield of cellulose nanoparticles also increases, when the enzyme dose exceeds 200U / g, the yield decreases. Therefore, to ensure optimal nanocellulose yield, the enzyme dose is 200 U / g.

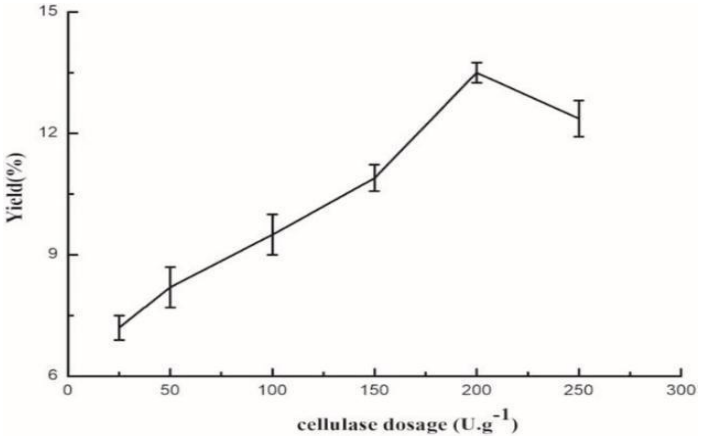

Figure 32. Effect of enzyme dose on nanoparticle yield. Figure adopted from Zhang et al. [63].

Figure 33 shows the timing of the enzymatic hydrolysis affects the final outcome. After 12 hours, the yield is optimal, however, because the reaction time is extended, the nanocellulose hydrolyzes to glucose lowers the yield. Due to limited binding sites, yields of cellulose nanoparticles tend to stabilize after 16 hours of enzymatic hydrolysis [63]

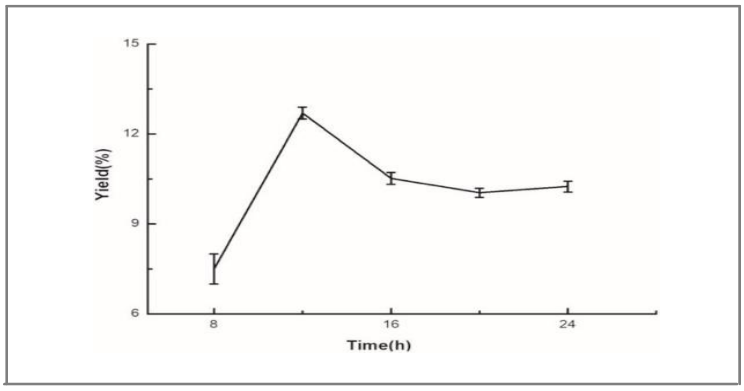

Figure 33. Effect of time on hydrolysis. Figure adopted from Zhang et al [63].

Figure 34a shows that temperature has a great influence on the result of enzymatic hydrolysis. The optimal temperature is 50°C. Below this temperature, enzyme activity slows down, resulting in lower yields. Beyond this temperature the enzymes become inactive, therefore, a gradual decrease in yield was observed [63]. The mean particle size of the sample is shown in Figure 34b. Sonication plays an important role in particle size. The average particle size of the sonicated nanocelluloses was 1600 nm, whereas the sonicated nanocelluloses were. The particle size is significantly reduced. Enzymatic hydrolysis temperature also affects the average particle size. At 40°C, the average particle diameter was 674 nm. When the enzymatic hydrolysis temperature increases to 50°C, the particle diameter decreases to 310 nm. However, at 60°C, the mean particle size increased to 565 nm due to changes in enzyme activity. Enzymatic hydrolysis and optimal particle size were obtained at 50°C [63].

Figure 34c shows the zeta potential of the sample is negative. The sample surface is negatively charged in the water. The absolute value of cellulose nanoparticles that were not sonicated was 21 mV, lower than that of the cellulose nanoparticles treated with sonication. Enzymatic hydrolysis temperature has little effect on zeta potential, but the optimal value is obtained at 50°C [63].

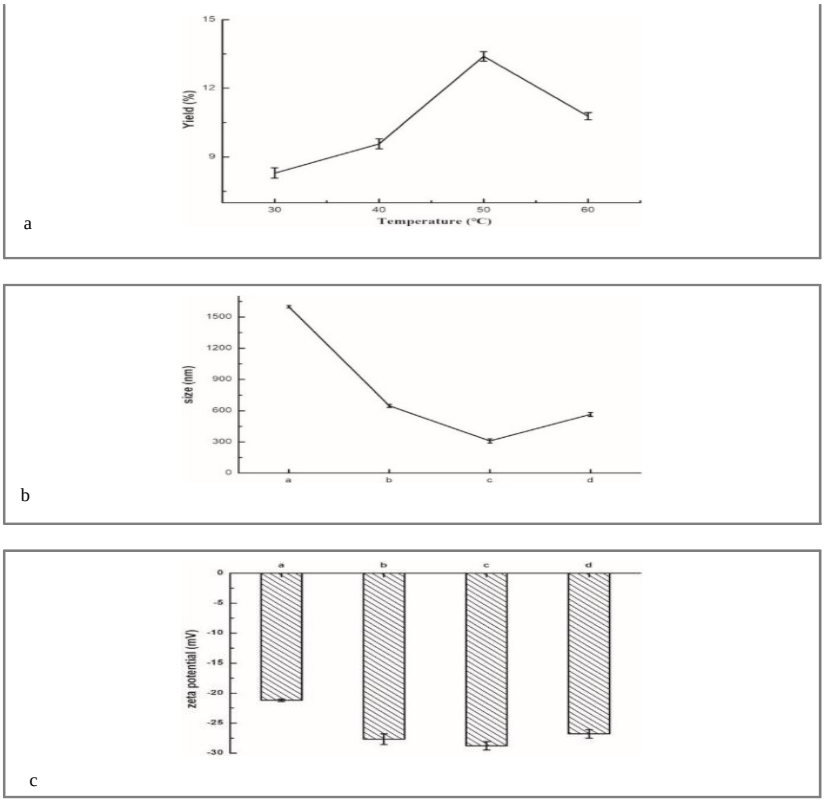

Figure 34. (a) Effect of temperature on enzymatic hydrolysis, (b) mean particle size of nanocellulose from enzymolysis at 50 without sonication at temperature 40 and by sonication at temperature 50-70. (c) zeta potential enzymolysis temperature 50 without sonication at temperature 40 and by sonication at temperature 50-70. Figure adopted from Zhang et al [63].

The chemical composition, crystallinity, and morphology of the composites were all characterized using FT-IR, x-ray diffraction, and TEM showing that the structure was not destroyed during the preparation process so that the crystal form remained in the form of cellulose I. The crystallinity was 61.98%, more 9.15% higher compared to poplar cellulose. Width between 20 and 50 nm [63].

2.6. Synthesis of Crystalline Nanocellulose from Cotton Fiber by Controlled Microbial Hydrolysis

For the synthesis of CNC from microcrystalline cellulose, the fibrous fungus *Trichoderma reesei* under controlled hydrolysis was used [34]. First of all, the raw material (cotton fiber) is converted into microcrystalline cellulose (MCC). Furthermore, MCC was hydrolyzed using microbes (*Trichoderma reesei or Acetobacter xylinum*) to produce CNC [34,64]. In the production of CNC, a 24-hour inoculum of the fungus *Trichoderma reesei* (ATCC 13631), was prepared in potato dextrose broth by inoculating the spore suspension (3 106 spores/ml). The optimized inoculum concentration was then added with Mandel Media containing MCC as the only carbon source. The next step was incubation at 25 °C under vibrating conditions of 150 rpm [64].

Synthesis using the fungus *Trichoderma reesei* does not produce peroxidase but produces cellulase which can degrade cellulose [34,64]. So that *Trichoderma reesei* is a good option for CNC production. By using the cellulase-free enzyme mechanism to break down cellulose, the carbohydrate-binding module (CBM) will combine with the flexible linker to form a multicomponent enzyme system that works synergistically to form crystalline cellulose. In order to increase the product obtained, the fermenter system is connected to a membrane to trap the resulting nanocrystalline [34].

The synthesis of nanocellulose by enzymatic methods makes it possible to make nanocellulose react with impurities. Thus, the purification of the CNC obtained by enzymatic processes is an important step in the production of CNC by this method. The production of CNC by microbial hydrolysis of MCC by the fungus *Trichoderma reesei* includes fermentation and differential centrifugation of the broth for sedimentation of all particles larger than 1 mm in size. The resulting supernatant is filtered through a 100 kDa ultrafiltration membrane, sucked in a vacuum where water and low molecular weight solutes pass through the membrane, CNC will be stuck on the membrane surface and removed by ultrapure water jets. Thus, differential centrifugation is combined with ultrafiltration. This enzymatic method using *Trichoderma reesei* is one of the best biological pathways in CNC synthesis. After purification, CNC was analyzed by Atomic Force Microscopy (AFM) to determine morphology and size. Figure 35 shows the morphology of CNC produced by microbial hydrolysis [34].

Meanwhile, Figure 36 shows the size distribution of crystalline nanocellulose obtained from the particle light scattering analysis. It can be seen from Figure 36 that the resulting crystalline nanocellulose has a diameter in the range of 100-150 nm and shows that there are also some whose sizes exceed 500nm

but this with low intensity is due to the purification method that has been carried out [34].

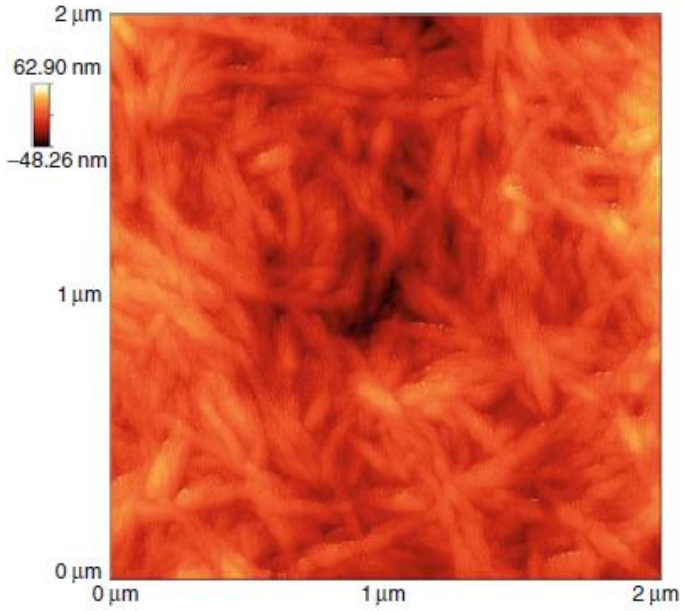

Figure 35. Morphology of crystalline nanocellulose through Atomic Force Microscopy (AFM) analysis. Figure adopted from Vigneshwaran et al. [34].

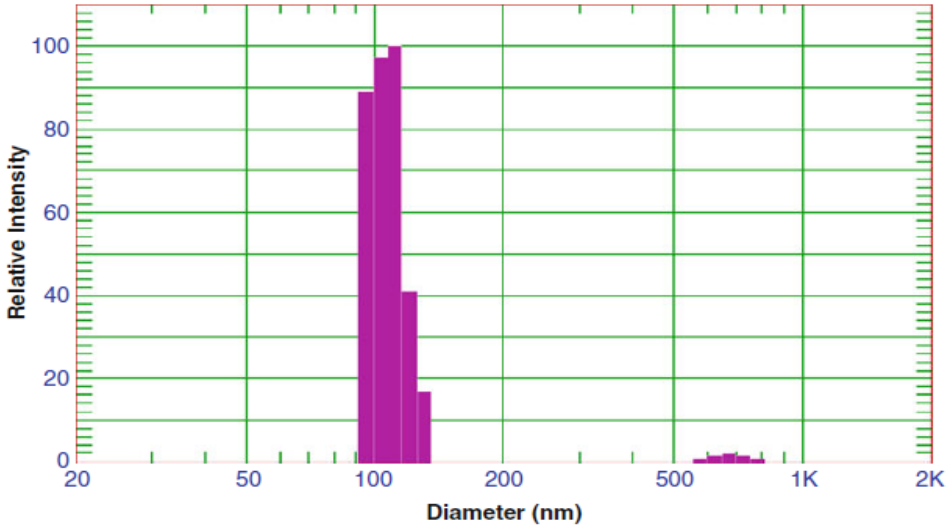

Figure 36. Distribution of crystalline nanocellulose synthesized by microbial hydrolysis. Figure adopted from Vigneshwaran et al. [34].

One of the best industries that produce nanocellulose, type of product, capacity and method in the world comes from Sweden. The company gives more research supported by Holmen pulp and paper SP technical research institute of Sweden, produces crystalline nanocellulose with a production capacity of 0.1 tonnes/day and is a pilot for the first half of 2016, while the production methods are controlled sulfuric acid and sonification washing based on technology by Melodea [28].

Conclusion

This review presents studies on the preparation, synthesis, and characterization of crystalline nanocelluloses as well as methods commonly used on an industrial scale related to crystalline nanocelluloses. To obtain crystalline nanocellulose as discussed earlier, biomass (OPEFB, Jalar leaves, pineapple fiber, bark tree fronds, shallot waste, and rice husks) are treated beforehand so that microcellulose is obtained which will then be hydrolyzed using various approaches such as the one has been shown above and obtained crystalline nanocellulose. Each approach presented in this review has its own advantages and disadvantages. However, an approach that is often applied on an industrial scale in accordance with the above study is strong acid hydrolysis. This is supported by TAPPI data in 2015, with the highest amount obtained is 0.1 tonnes/day. In addition, the production time in the synthesis of crystalline nanocellulose is relatively short compared to other studies. Thus, the authors argue that acid hydrolysis is a relevant way to be applied on an industrial scale crystalline nanocellulose apart from the weaknesses of this method which also becomes a consideration for developing a more efficient method.

References

[1] N. K. Maddahy, O. Ramezani, and H. Kermanian, Production of nanocrystalline cellulose from sugarcane bagasse, Proceedings of the 4th International Conference on Nanostructures (ICNS4) 12-14 March, Kish Island, I. R. Iran, (2012)

[2] A. Mandal, D. Chakrabarty, Isolation of nanocellulose from waste sugarcane bagasse (SCB) and its characterization; *Carbohydrate Polymers*, 86(3): 1291-1299 (2011)

[3] M. E. Himmel, S. Y. Ding, D. K. Johnson, W. S. Adney, M. R. Nimlos, J. W. Brady, and T. D. Foust, Biomass recalcitrance: engineering plants and enzymes for biofuels production*; Science*, 315(80): 804-807 (2007)

[4] L. Jasmani and W. Thielemans, Preparation of nanocellulose and its potential application; *Forest Research*, 7(3): 2 (2018)

[5] Li, Wei, Yue. J, and Liu, Preparation of nanocrystalline cellulose via ultrasound and its reinforcement capability for poly (vinyl alcohol) composites; *Ultrasonics Sonochemistry*, 19(3): 479-485 (2012)

[6] V. Favier, G. R. Canova, J. Y. Cavaillé, H. Chanzy, A. Dufresne, and C. Gauthier, Nanocomposite materials from latex and cellulose whiskers; *Polymers for Advanced Technologies*, 6(5): 351-355 (1995)

[7] I. A. Sacui, R. C. Nieuwendaal, D. J. Burnett, S. J. Stranick, M. Jorfi, C. Weder, E.J. Foster, R.T. Olsson, and J.W. Gilman, Comparison of the properties of cellulose nanocrystals and cellulose

nanofibrils isolated from bacteria, tunicate, and wood processed using acid, enzymatic, mechanical, and oxidative methods; *American Chemical Society Applied Materials and Interfaces,* 6 (9): 6127-6138 (2014)

[8] C. P. Chang, I. C. Wang, K. J. Hung, Y. S. Perng, Preparation and characterization of nanocrystalline cellulose by acid hydrolysis of cotton linter; *Taiwan Journal for Science,* 25(3): 64-251 (2010)

[9] W. Helbert, J.Y. Cavaille, A. Dufresne, Thermoplastic nanocomposites filled with wheat straw cellulose whiskers. Part I: processing and mechanical behavior; *Polymer composites,* 17(4): 604-611 (1996)

[10] A. Bendahou, Y. Habibi, H. Kaddami, and A. Dufresne, Preparation of cellulose whiskers and natural rubber-based nanocomposites; *Journal of Biobased Materials and Bioenergy,* 3: 81-90. (2009)

[11] B. Brito, F. Pereira, J. Putaux, and B. Jean, Preparation, morphology and structure of cellulose nanocrystals from bamboo fibers; *Cellulose,* 19: 1527-1536 (2012)

[12] J. Zhang, Y. Wang, L. Zhang, R. Zhang, G. Liu, and G. Cheng, Understanding changes in cellulose crystalline structure of lignocellulosic biomass during ionic liquid pretreatment by XRD; *Bioresource Technology,* 151: 402-405 (2014).

[13] D. Bondenson, A. Mathew, and K. Oksman, Optimization of the isolation of nanocrystals from microcrystalline cellulose by acid hydrolysis; *Cellulose,* 13(2): 171 (2006).

[14] M. Ioelovich, Optimal conditions for isolation of nanocrystalline cellulose particles; *Nanoscience and Nanotechnology,* 2(2): 9-13 (2012)

[15] Y. Habibi, and A. Dufresne, Highly filled bionanocomposites from functionalized polysaccharide nanocrystal; *Biomacromolecules,* 9(7): 1974-1980 (2008)

[17] E. Fortunati, S. Rinaldi, M. Peltzer, N. Bloise, L. Visai, I. Armentano, and J. M. Kenny, Nano-biocomposite films with modified cellulose nanocrystals and synthesized silver nanoparticles, *Carbohydrate Polymers,* 101: 1122-1133 (2014)

[16] L. H. Zaini, M. Jonoobi, P.M. Tahir, and S. Karimi, Isolation and characterization of cellulose whiskers from kenaf (Hibiscus cannabinus L.) bast fibers; *Journal of Biomaterials and Nanobiotechnology,* 4(1): 8 (2013)

[18] R.M. Sheltami, I. Abdullah, I. Ahmad, A. Dufresne, and H. Kargarzadeh, Extraction of cellulose nanocrystals from mengkuang leaves (Pandanus tectorius); *Carbohydrate Polymers,* 88(2): 772-779 (2012)

[19] N. L. Garcia de Rodriguez, W. Thielemans, and A. Dufresne, Sisal cellulose whiskers reinforced polyvinyl acetate nanocomposites; *Cellulose,* 13(3): 261–270 (2006)

[20] M. N. Angles, and A. Dufresne, Plasticized starch/tunicin whiskers nanocomposites. 1.Structural analysis; *Macromolecules,* 33.22: 8344-8353 (2000)

[21] A. Hirai, O. Inui, F. Horii, and M. Tsuji, Phase separation behavior in aqueous suspensions of bacterial cellulose nanocrystals prepared by sulfuric acid treatment; *Langmuir* 25(1): 497-502 (2009)

[22] J. George, A.S. Bawa, and Siddaramaiah, Synthesis and characterization of bacterial cellulose nanocrystals and their PVA nanocomposites; *Advanced Materials Research,* 123: 383-386 (2010)

[23] R. P. Swatloski, S. K. Spear, J. D. Holbrey, R. D. Rogers, Dissolution of cellulose with ionic liquids; *Journal of the American Chemical Society*, 124(18): 4974–4975 (2002)

[24] W. Li, J. Yue, Liu, S. Preparation of nanocrystalline cellulose via ultrasound and its reinforcement capability for poly (vinyl alcohol) composites; *Ultrasonics Sonochemistry,* 19: 479-485 (2012)

[25] B. L. Peng, N. Dhar, H. L. Liu, and K. C. Tam, Chemistry and applications of nanocrystalline cellulose and its derivatives: a nanotechnology perspective; *Canadian Journal of Chemical Engineering,* 89: 1191-1206 (2011)

[26] H. M. A. Ehmann, T. Mohan, M. Koshanskaya, S. Scheicher, D. Breitwieser, V. Ribitsch, K. Stana-Kleinschek, and S. Spirk, Design of anticoagulant surfaces based on cellulose nanocrystals; *Chemical Communication*, 50 (86): 13070–13072 (2014)

[27] M. Mariano, N. El Kissi, and A. Dufresne, Cellulose nanocrystals and related nanocomposites: review of some properties and challenges; *Journal of Polymer Science Part B Polymer Physics*, 52(12): 791–806 (2014)

[28] M. Rajinipriya, M. Nagalakshmaiah, M. Robert, and Elkoun, importance of agricultural and industrial waste in the field of nanocellulose and recent industrial developments of wood based nanocellulose: A review; *American Chemical Society Sustainable Chemistry and Engineering*, 6: 2807–2828 (2018)

[29] Y. Chen, C. Liu, P. R. Chang, X. Cao, and D. P. Anderson, Bionanocomposites based on pea starch and cellulose nanowhiskers hydrolyzed from pea hull fibre: Effect of hydrolysis time; *Carbohydrate Polymers*, 76 (4): 607-615 (2009)

[30] N. Wang, E. Ding, and R. Cheng, Thermal degradation behaviors of spherical cellulose nanocrystals with sulfate groups; *Polimer* 48 (12): 3486-3493 (2007)

[31] Y. Zheng, Z. Pan, R. Zhang, Overview of biomass pretreatment for cellulosic ethanol production; *International Journal of Agricultural and Biological Engineering*, 2(3): 51-68 (2009)

[32] O. Sanchez, R. Sierra, C.J. Almeciga-Dıaz, Delignification process of agro-industrial wastes an alternative to obtain fermentable carbohydrates for producing fuel; *Maximino Manzanera,* 111-138

(2011).

[33] Z. Man, M. Nawshad, S. A. B. Ariyanti, Mohamad, K. M. Vignesh, R. Sikander, Preparation of cellulose nanocrystals using an ionic liquid; *Journal of Polymer and the Environment*, 19: 726-731 (2011)

[34] N. Vigneshwaran, P. Satyamurthy, and P. Jain, Biological synthesis of nanocrystalline cellulose by controlled hydrolysis of cotton fibers and linters; *Handbook of Polymer Nanocomposites. Processing, Performance and Application. Springer-Verlag Berlin Heidelberg*, 27–36 (2014).

[35] Z. Y. Qin, G. Tong, Y. C. Frank Chin, and J. Zhou, Preparation of ultrasonic-assisted high carboxylate content cellulose nanocrystals by TEMPO oxidation; *BioResources*, 6(2): 1136-1146 (2011).

[36] J. Rojas, M. Bedoya, and Y. Ciro, Current trends in the production of cellulose nanoparticles and nanocomposites for biomedical applications; *Cellulose- Fundamental Aspects Current Trends*, 197-198 (2015) doi:10.5772/61334. https://www.intechopen.com/books/cellulose-fundamental-aspects-and-current-trends/current-trends-in-the-production-of-cellulose-nanoparticles-and-nanocomposites-for-biomedical-applic

[37] D. Klemm, T. Helme, B. Philipp, and W. Wagenbiecht, New approaches to advanced polymers by selective cellulose functionalization; *Acta Polymerica*, 48(8): 277–297 (1997)

[38] Q. Xiang, Y. Y. Lee, P. O. Petterson, and R. W. Torget, Heterogeneous aspects of acid hydrolysis of α-cellulose; *Applied Biochemistry and Biotechnology - Part A Enzym. Eng. Biotechnol*, 107(1-3): 505–514 (2003).

[39] N. Johar, I. Ahmad, and A. Dufresne, Extraction, preparation and characterization of cellulose fibres and nanocrystals from rice husk; *Industrial Crops and Products*, 37(1): 93–99 (2012)

[40] J. I. Morán, V. A. Alvarez, V. P. Cyras, and A. Vázquez, Extraction of cellulose and preparation of nanocellulose from sisal fibers; *Cellulose*, 15: 149–159 (2008)

[41] M. E. Gibril, P. Lekha, J. Andrew, B. Sithole, T. Tesfaye, and D. Ramjugernath, Beneficiation of pulp and paper mill sludge: production and characterisation of functionalised crystalline nanocellulose; *Clean Technologies and Environmental Policy*, 20(8): 1835–1845 (2018)

[42] P. Lu, Y. Hsieh, and Y. Lo, Cellulose isolation and core-shell nanostructures of cellulose nanocrystals from chardonnay grape skins; *Carbohydrate Polymers*, 87(4): 2546–2553 (2012)

[43] R. M. Sheltami, I. Abdullah, I. Ahmad, A. Dufresne, and H. Kargarzadeh, Extraction of cellulose nanocrystals from mengkuang leaves (Pandanus tectorius); *Carbohydrate Polymers*, 88(2): 772–779 (2012)

[44] E. Putri, and S. Gea, Isolasi dan karakterisasi nanokistral selulosa dari tandan sawit (Elaeis

Guineensis Jack); *Elkawnie*, 4(1): 13–22 (2018)

[45] Sumaiyah, B. Wirjosentono, M. P. Karsono, Nasution, and S. Gea, Preparation and characterization of nanocrystalline cellulose from sugar palm bunch (Arenga pinnata (Wurmb) Merr.); *International Journal of PharmTech Research*, 6(2): 814–820 (2014)

[46] Triapriani, Pembuatan nanoselulosa dari tandan kosong sawit dengan metode hidrolisis asam. Fakultas Matematika dan Ilmu Pengetahuan Alam Universitas Lampung: Bandar Lampung. (2016).

[47] L. Triyastiti, and D. Krisdiyanto, Isolasi Nanokristal Selulosa Dari Pelepah Pohon Salak Sebagai Filler Pada Film Berbasis Polivinil Alkohol (PVA); *Indonesian Journal of Materials Chemistry*, 1(1): 39-45 (2018)

[48] A. M. Adel, Z. H. A. El-Wahab, A. A. Ibrahim, and M. T. Al-Shemy, Characterization of microcrystalline cellulose prepared from lignocellulosic materials. Part 1. Acid catalyzed hydrolysis; *Bioresource Technology*,101(12): 4446-4455 (2010)

[49] Li, Wei, J. Yue, and S. Liu, Preparation of nanocrystalline cellulose via ultrasound and its reinforcement capability for poly (vinyl alcohol) composites; *Ultrasonics Sonochemistry*, 19.3: 479-485 (2012)

[50] I. G. M. Sanjaya, Ekstraksi dan karakterisasi nanoselulosa dari limbah kulit bawang merah; *Journal Education and Chemistry*, 2(2): 77–81 (2020)

[51] D. A. P. Husni, E. A. Rahim, and R. Ruslan, Pembuatan membran selulosa asetat dari selulosa pelepah pohon pisang; *KOVALEN: Jurnal Riset Kimia*, 4(1): 41–52 (2018)

[52] Purwanti, Endah, and S. Dampang, Pengaruh perbedaan kondisi hidrolisis terhadap hasil isolasi nanokristalin selulosa dari bonggol jagung; *Indonesian Journal of Chemical Research*, 5(1): 12-16 (2017)

[53] S. D. Pandiangan, Sintesa dan karakterisasi nanokristal selulosa serat eucalyptus pellita yang terhornifika; *Universitas Sumatra Utara*, 16-41(2019).

[54] R. Li, J. Fei, Y. Cai, J. Feng, and J. You, Cellulose whiskers extracted from mulberry: A novel biomass production; *Carbohydrate Polymers*, 76(1): 94–99 (2009).

[55] H. Onggo, W. Subowo, Sudirman, Analisis sifat termal komposit polipropilen-kenaf; *Prosiding Simposium Nasional Polimer V P2F-LIPI*, 140–156 (2005)

[56] J. L. Minor, Hornification -Its origin and meaning; *Progress in Paper Recycling*, 3(2): 93–95 (1994).

[57] A. Solikhin, Y. S. Hadi, M. Y. Massijaya, and S. Nikmatin, Morphological, chemical, and thermal characteristics of nanofibrillated cellulose isolated using chemo-mechanical methods; *Makara Journal of Science*, 21(2): 59-68 (2017)

[58] D. B. Effendi, N. H. Rosyid, A. B. D. Nandiyanto, A. Mudzakir, Review: Sintesis Nanoselulosa;

Jurnal Integrasi Proses, 2(5): 61-74 (2015)

[59] S. Montanari, M. Roumani, L. Heux, and M. R. Vignon, Topochemistry of carboxylated cellulose nanocrystals resulting from TEMPO-mediated oxidation; *Macromolecules* 38(5): 1665-1671 (2005)

[60] M. Yahya, H. V. Lee, and Sharifah, Preparation of nanocellulose via transition metal salt-catalyzed hydrolysis pathway; *BioResources*, 10(4): 7627-7639 (2015)

[61] M. Grube, J. G. Lin, P. H. Lee, and S. Kokorevicha, Evaluation of sewage sludge-based compost by FT-IR spectroscopy; *Geoderma*, 130(3-4): 324–333 (2006)

[62] E. Smidt, K. U. Eckhardt, P. Lechner, H. R. Schulten, and P. Leinweber, Characterization of different decomposition stages of biowaste using FT-IR spectroscopy and pyrolysis-field ionization mass spectrometry; *Biodegradation*, 16: 67–79 (2005).

[63] Y. Zhang, J. Chen, L. Zhang, P. Zhan, N. Liu, and Z. Wu, Preparation of nanocellulose from steam exploded poplar wood by enzymolysis assisted sonication; *Material Research Express* 7(3): 1-8 (2020).

[64] Á. T. Martínez, M. Speranza, F. J. Ruiz-Dueñas, P. Ferreira, S. Camarero, F. Guillén, M. J. Martínez, A. Gutiérrez, and J. C. Del Río, Biodegradation of lignocellu-losics: microbial, chemical, and enzymatic aspects of the fungal attack of lignin; *International Microbiology*, 8(3): 195–204 (2005)
